doi: 10.1590/S0102-261X1997000200003

NUMERICAL INVERSION OF TWO-DIMENSIONAL GEOELECTRIC CONDUCTIVITY DISTRIBUTIONS FROM MAGNETOTELLURIC DATA

H. F. de C. Velho & F. M. Ramos

In this paper, a new inversion technique, called the minimum first-order entropy (MinEnt-1) method, is proposed for the reconstruction of two-dimensional geoelectric conductivity distributions from magnetotelluric (MT) data. The method combines an iterative search with a regularization technique based on the minimization of the entropy measure of the vector of first-differences of the unknown conductivities. Numerical simulations, using synthetic data corrupted with gaussian noise, show that the MinEnt-1 algorithm converges to excellent conductivity reconstructions, yielding in many cases results that are superior to those obtained by the maximum entropy formalism. Unlike other classical regularization schemes, which maximize smoothness for a given data, the proposed method constrains the class of possible solutions into a restricted set of low entropy models, constituted by locally smooth regions separated by sharp discontinuities. This may be an effective approach for the incorporation of prior information about the local smoothness of the real physical model.

Key words: Magnetotelluric inversion; Optimization; Entropic regularization.

INVERSÃO NUMÉRICA DE DISTRIBUIÇÕES BIDIMENSIONAIS DE CONDUTIVIDADE GEOELÉTRICA A PARTIR DE DADOS MAGNETOTELÚRICOS - *Neste trabalho, propõe-se uma nova técnica de inversão, chamada de método da mínima entropia de primeira ordem (MinEnt-1), para reconstrução de distribuições bidimensionais de condutividade geoelétrica, a partir de dados magnetotelúricos (MT). O método combina uma busca iterativa com uma técnica de regularização baseada na minimização da medida de entropia do vetor de diferenças primeiras das condutividades a serem estimadas. Simulações numéricas, com a utilização de dados sintéticos contaminados com ruído gaussiano, mostram que o algoritmo MinEnt-1 produz excelentes reconstruções de condutividade, com resultados melhores que os obtidos pelo método da máxima entropia. Diferentemente dos outros esquemas clássicos de regularização, que maximizam suavidade para um dado conjunto de dados, o método proposto limita a classe de possíveis soluções a um conjunto restrito de modelos de baixa entropia, constituído por regiões localmente lisas separadas por descontinuidades abruptas. Esta abordagem pode ser bastante eficaz para incorporação de informação a priori sobre a natureza da suavidade local do modelo físico real.*

Palavras-chave: *Inversão magnetotelúrica; Otimização; Regularização entrópica.*

Laboratório Associado de Computação e Matemática Aplicada (LAC)
Instituto Nacional de Pesquisas Espaciais (INPE)
Caixa Postal 515 - 12201-970 - São José dos Campos - SP - Brasil
Tel.: (012) 3456356 - Fax: (021) 3456375

INTRODUCTION

The use of electromagnetic fields induced by natural sources in the ionosphere and magnetosphere to determine the electrical conductivity of the earth's subsurface has a wide range of applications in geophysics. Appearing in various areas such as petroleum prospection, mining and search for groundwater, this inverse problem, also known as inversion of magnetotelluric (MT) data, has special relevance in the exploration of regions which are difficult to probe with conventional seismic methods. These areas usually involve either near-surface basalt layers, which cause very strong reflections, or regions where tectonic events have disrupted the sedimentary layer geometries and greatly complicated the seismic signature (Madden & Mackie, 1989).

Independently proposed by Tikhonov (1950) and Cagniard (1953), the MT method is based on the computation of transfer functions between the electric and magnetic fields measured at the earth's surface. These transfer functions define a frequency dependent tensor impedance which expresses an assumed linear relationship between the geomagnetic field and the resulting electric fields in the earth. The observation depth of a given measurement is dependent upon the frequency of the detected signal and upon the subsurface conductivity. Low-frequency electromagnetic waves penetrate more deeply than do high-frequency waves, whereas waves of a given frequency penetrate deeper into resistive rocks than into conductive rocks. The final step in a MT study is to interpret the computed data in terms of rock type and geologic structures as a function of position and depth. This quantitative interpretation is based on the mathematical inversion of impedance versus frequency into the resistivity versus depth form.

The MT inversion problem has been the subject of several studies and two excellent reviews have been published by Oldenbur (1990) and Raiche (1994). Inversion algorithms of MT data usually involve a systematic search for the earth model which best fits the observed data. The inversion proceeds by minimizing an objective functional which includes the difference between the observed and the predicted data and a regularization function. The regularization term expresses the prior assumptions about the geology, and allows to reduce the presence of artifacts in the conductivity models reconstructed from sparse, noisy MT data sets. Constable et al. (1987), deGroot-Hedlin & Constable (1990), Smith & Brooker (1988, 1991), Oldenburg & Ellis (1991) have used this approach to obtain minimum structure conductivity models for the MT inverse problem. In a formulation that resembles the regularization method developed by Phillips (1962), Tikhonov (1963) and Twomey (1963), minimum structure models are obtained with the help of a "smoothing" operator which essentially performs a numerical first or second derivative on the conductivies, and explicitly suppress complexity from the inverse solutions.

In this study, a new regularization approach is introduced based on the minimization of the entropy measure of the vector of *first-differences* of the unknown parameters. The MT inversion is formulated as a constrained nonlinear optimization problem and solved by a quasi-Newtonian minimization algorithm. The minimization of the first-order entropy measure of the vector of parameters constrains the class of candidate solutions into a restricted set of models composed by locally smooth regions separated by sharp discontinuities. The next section presents a brief presentation of the formulation of the forward problem. This is followed by a description of the proposed inversion method, and a discussion of the numerical examples. The method is tested over two-dimensional earth models embedded with conductivity discontinuities, using synthetic data corrupted with gaussian noise.

FORMULATION OF THE FORWARD PROBLEM

The commom approaches for solving the forward problem involve analytical methods, boundary or volume integral methods, Fourier methods, finite difference methods, finite element methods and hybrid techniques (Jupp & Vozoff, 1977; Madden & Mackie, 1989). The choice of a method is a matter of speed, accuracy, and simplicity. In this study, to perform the forward calculations required by the inversion scheme, a finite difference code, based on the two-dimensional conductivity inhomogeneity model proposed by Jones & Price (1970), has been used.

The mathematical formulation of the problem is given by Maxwell's equations in a two-dimensional region with suitable boundary conditions. Schematically, the problem domain is depicted in Fig. 1, where Ω+ and Ω- correspond to the conductive zone ($z < 0$) and the free-space zone ($z >$

0), respectively. The oscillating field has period $2\pi/\omega$ sufficiently long to permit displacement currents being ignored. The magnetic permeability is taken as unity. The equations are therefore

$$\vec{\nabla} \times \vec{H} = 4\pi\sigma \vec{E} \tag{1}$$

and

$$\vec{\nabla} \times \vec{E} = -i\omega \vec{H}, \tag{2}$$

where the time factor exp $(i\omega t)$ is assumed in all field quantities, and $\sigma = \sigma(y, z)$ is the electric conductivity.

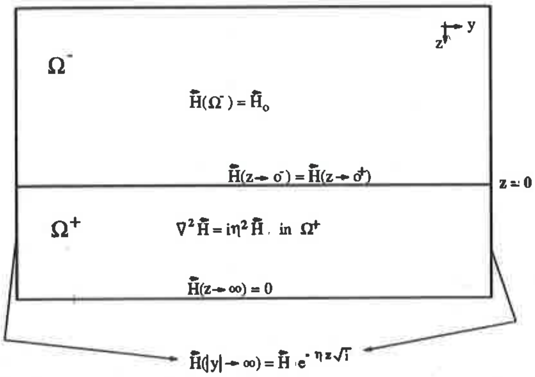

Figure 1 - Geometry and boundary conditions of the forward problem.

Figura 1 *- Geometria e condições de contorno do problema direto.*

Since $\vec{H}$ and $\vec{E}$ are independent of the strike direction x, Eqs. (1) and (2) take the form of two sets of equations

$$\begin{cases} \partial H_z/\partial y - \partial H_y/\partial z &= 4\pi\sigma E_x \\ \partial H_x/\partial z &= 4\pi\sigma E_y \\ -\partial H_x/\partial y &= 4\pi\sigma E_z \end{cases} \tag{3}$$

and

$$\begin{cases} \partial E_z/\partial y - \partial E_y/\partial z &= -i\omega H_x \\ \partial E_x/\partial z &= -i\omega H_y \\ -\partial E_x/\partial y &= -i\omega H_z, \end{cases} \tag{4}$$

which can be solved separately.

Eliminating H_y and H_z from Eq. (3), the transverse electric (TE) mode equations (*E-polarization* problem) are obtained:

$$\vec{\nabla}^2 E_x = \frac{\partial^2 E_x}{\partial y^2} + \frac{\partial^2 E_x}{\partial z^2} = i\eta^2 E_x, \tag{5}$$

$$\partial E_x/\partial z = -i\omega H_y \tag{6}$$

and

$$-\partial E_x/\partial y = -i\omega H_z, \tag{7}$$

where

$$\eta^2 = 4\pi\sigma\omega. \tag{8}$$

Similarly, eliminating E_y and E_z from Eq. (4), the transverse magnetic (TM) mode equations (*H-polarization* problem) are given as

$$\vec{\nabla}^2 H_x = \frac{\partial^2 H_x}{\partial y^2} + \frac{\partial^2 H_x}{\partial z^2} = i\eta^2 H_x, \tag{9}$$

$$\partial H_x/\partial z = 4\pi\sigma E_y \tag{10}$$

and

$$-\partial H_x/\partial y = 4\pi\sigma E_z. \tag{11}$$

MT data can be characterized by TE and TM mode impedances, given respectively by

$$Z_{xy} = \frac{E_x}{H_y} \tag{12}$$

and

$$Z_{yx} = \frac{E_y}{H_x}, \tag{13}$$

or by apparent resistivities and phase of the form

$$\rho_a = \frac{1}{\mu_0\omega}|Z|^2 \tag{14}$$

and

$$\phi = \arg(Z), \tag{15}$$

where Z refers to Z_{xy} and Z_{yx} for the TE and TM modes, respectively.

Although true 2D inversion embraces both polarizations (Jupp & Vozoff, 1977), for the sake of simplicity only the *H-polarization* problem will be considered in the following analysis.

Boundary Conditions

It is assumed that the conductive inhomogeneities embedded in Ω+ are sufficiently small to permit the medium to behave like a uniform conductor at large distances of the discontinuities in σ. Hence, as $y \to \pm \infty$ Eq. (9) becomes

$$\frac{\partial^2 H_x}{\partial z^2} = i\eta^2 H_x \qquad (16)$$

and the field tends to zero for large positive values of z. Therefore, the appropriate solution of Eq. (16) is

$$H_x = H_0 e^{-\eta z\sqrt{i}}. \qquad (17)$$

Across the interfaces between Ω+ and Ω- ($z = 0$) and between different media within the conductive region, H_x is continuous. Outside the conductor, where $\sigma = 0$, H_x is independent of y and z.

Numerical Formulation

Splitting the magnetic field into its real and imaginary componentes, $\vec{H} = \vec{F} + i\vec{G}$, Eq. (9) can be written as

$$\nabla^2 H = \nabla^2 F + i\nabla^2 G = (-\eta^2 G) + i\,(\eta^2 F) \qquad (18)$$

and

$$\nabla^2 \Phi = i\eta^2 M\Phi \qquad (19)$$

with

$$\Phi = \begin{bmatrix} F \\ G \end{bmatrix}, \quad M = \begin{bmatrix} 0 & -1 \\ 1 & 0 \end{bmatrix}.$$

Approximating Eq. (19) by finite differences over a two-dimensional nonuniform grid of rectangular prisms, each one having a uniform electrical conductivity $\sigma_{j,k}$, the resulting system of algebraic equations can be iteratively solved by the Gauss-Seidel method (Hoffman, 1993, pp. 53-54).

A computer code was written based on the above calculation procedure, and validated against the results presented by Jones & Price (1970).

FORMULATION OF THE INVERSE PROBLEM

The vector of conductivities to be determined by the inverse analysis is denoted by

$$\mathbf{p} = \{p_1, p_2, ..., p_q, ... p_Q\} = \{\sigma_{11}, \sigma_{21}, ..., \sigma_{jk}, ... \sigma_{JK}\},$$

where $q = J(k-1) + j$, with $j = 1, ..., J$ and $k = 1, ..., K$. The MT inversion can be formulated as a nonlinear constrained minimization problem,

$$\min J(\mathbf{p}),\ l_q \le p_q \le u_q,\ q = 1, ..., Q, \qquad (20)$$

where

$$J(\mathbf{p}) = R(\mathbf{p}) - \gamma_0 S_0(\mathbf{p})/S_{max} + \gamma_1 S_1(\mathbf{p})/S_{max}, \qquad (21)$$

S_0 and S_1 are regularization functions, γ_0 and γ_1 are positive regularization parameters, and S_{max} a normalization constant. The bounds l_q and u_q are chosen to allow the inversion to lie within some a priori known plysical limits.

The misfit between model and data is given by

$$R(\mathbf{p}) = \sum_{j=1}^{N_y} \sum_{m=1}^{M} \left[\Phi^E_{j,m} - \Phi^C_{j,m}(\mathbf{p})\right]^2, \qquad (22)$$

with the superscripts E and C denoting the experimental and computed data, respectively. It is assumed that measurements $\Phi^E_{j,m}$ are available at $j = 1, 2, ..., N_y$ horizontal positions and at ω_m, $m = 1, 2, ..., M$, different frequencies. Considering that the magnetic field for the TM mode is constant at $z = 0$, the inversion algorithm is fed with H_x values predicted by the forward model one horizontal grid line *below* the earth's surface. This is equivalent of using a first-order finite difference approximation of Eq. (10) for computing Z_{yx}, at $z = 0$.

The choice of the regularization function and of the regularization parameters will be discussed in the next section.

Minimum First-Order Entropy Regularization

It is well known that observational data is generally insufficient to provide a unique and stable solution when tackling an inverse problem. The recommended approach in this case is the use of any regularization technique, in order to assure that parameter variations are bounded to such a degree that the final solution looks physically reasonable (Pilkinton & Todoeschuck, 1991). Generally, this rather vague notion of reasonable means in fact smoothness. In other words, classical regularization techniques, such as Tikhonov's regularization and the maximum entropy formalism, search for *global* regularity and yield the smoothest reconstructions which are consistent with the available data.

The maximum entropy principle was first proposed as a general inference procedure by Jaynes (1957) on the basis of Shannon's axiomatic characterization of the amount of information (Shannon & Weaver, 1949). The maximum entropy principle has successfully been applied to a variety of fields including radioastronomy (Gull & Daniel, 1978), tomography (Smith et al., 1991), nondestructive testing (Ramos & Giovannini, 1995), pattern recognition (Fleisher et al., 1990) and crystallography (de Boissieu et al., 1991).

In this study, a new regularization approach is introduced based on the minimization of the entropy measure S_1 of the vector of *first-differences* of **p**. Adopting the standard terminology (Tikhonov & Arsenin, 1977), this regularization technique is called the *minimum first-order entropy* method (MINENT-1). Similarly, the maximum entropy method, which uses the zeroth-order entropy measure $S_0(\mathbf{p})$ as regularization function, is hereafter denoted by MAXENT-0. Therefore, the regularization functions in Eq. (21) are given by

$$S_\alpha(\mathbf{p}) = -\sum_{q=1}^{Q} s_q \log(s_q), \alpha = 0,1, \tag{23}$$

where

$$s_q = r_q \Big/ \sum_{q=1}^{Q} r_q \tag{24}$$

and

$$r_q = \begin{cases} p_q & \text{if } \alpha = 0 \\ |p_q - p_{q-1}| + \varsigma & \text{if } \alpha = 1, \end{cases} \tag{25}$$

ζ being a small positive constant (say, $\zeta = 10^{-15}$) which assures that the first-order entropy will always have a definite value. The function S_α attain its global maximum when all r_q are the same, which corresponds to a uniform distribution with a value of $S_{max} = \log Q$. On the other hand, the lowest entropy level, $S_{min} = 0$, is attained when all elements r_q but one are set to zero.

To illustrate the essential feature of the MINENT-1 method, Fig. 2 compares the normalized entropies $\bar{S}_0 = S_0/S_{max}$ of three different 1D models, represented by curves of normalized conductivity σ_i/σ_{max} as a function of i, where the index i refers to a depth z_i. Model **a** represents a uniformly conductive model, while models **b** and **c** contain each a resistive inclusion generated, respectively, by a smooth gaussian curve and a square-wave function. The results show that, although models **a**, **b** and **c** differ strongly, their zeroth-order entropy measures are all very close to unity. Looking now at the normalized first-differences $|\sigma_i - \sigma_{i-1}|/\sigma_{max}$ of models **a**, **b** and **c**, shown in Fig. 3, it can be seen that their normalized first-order

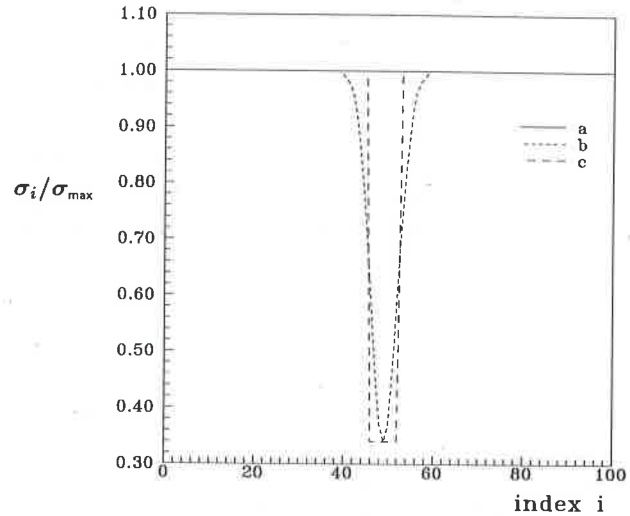

Figure 2 - Normalized models **a**, **b** and **c**, and respective normalized zeroth-order entropy values, $\bar{S}_0^a = 1.000$, $\bar{S}_0^b = 0.9969$ and $\bar{S}_0^c = 0.9955$.

Figura 2 *- Modelos normalizados* **a**, **b** *e* **c**, *e respectivos valores normalizados de entropia de ordem zero,* $\bar{S}_0^a = 1{,}000$, $\bar{S}_0^b = 0{,}9969$ and $\bar{S}_0^c = 0{,}9955$.

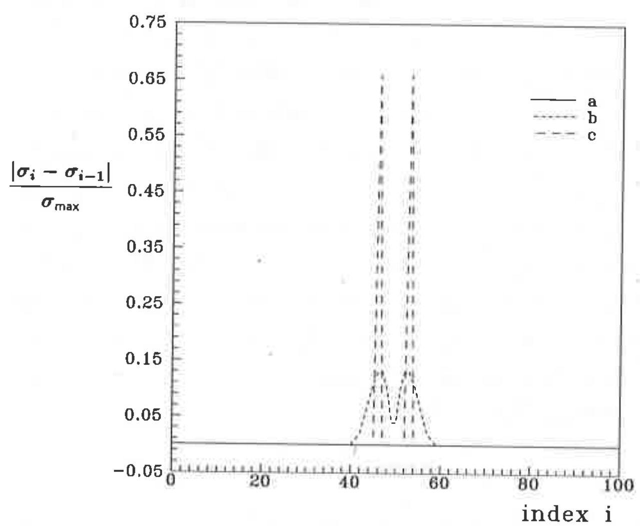

Figure 3 - Normalized first-differences of models **a**, **b** and **c**, and respective first-order entropy values, $\bar{S}_1^a = 1.000$, $\bar{S}_1^b = 0.5958$ *and* $\bar{S}_1^c = 0.1502$.

Figura 3 *- Diferenças primeiras normalizadas dos modelos* **a**, **b** *e* **c**, *e respectivos valores normalizados de entropia de primeira ordem,* $\bar{S}_1^a = 1{,}000$, $\bar{S}_1^b = 0{,}5958$ *and* $\bar{S}_1^c = 0{,}1502$.

entropy values $\bar{S}_1 = S_1/S_{max}$ present a much greater variability: $\bar{S}_1^a = 1.00$, $\bar{S}_1^b = 0.60$ and $\bar{S}_1^c = 0.15$. Moreover, it is possible to note that the sharper the discontinuity embedded in the model, the lower will be the value of its first-order entropy.

Clearly, while the existing regularization schemes, such as maximum entropy or Occam's inversion, search for "the smoothest model which fits the data to within an expected tolerance" (Constable et al., 1987), the MINENT-1 method looks for locally smooth regions separated by sharp discontinuities. Any reconstruction sharing these features has a high level of information and thus a low entropy content. Many geophysically interesting properties and structures may behave in a similar fashion.

The entropy concentration theorem (Jaynes, 1982) provides a quantitative justification for the MINENT-1 method. According to this theorem, the vast majority of all possible outcomes in a random experiment have frequency distributions close to uniform. In other words, distributions with low entroy levels are highly atypical. Therefore, if there is prior evidence on the low first-order entropy content of a geological structure in study, the MINENT-1 method leads to a drastic reduction in the number of candidate solutions (i.e., those which are consistent with the available data) to be iteratively probed by the inversion algorithm.

The value of the regularization parameter, which plays a role of a Lagrange-multiplier, is problem dependent. Since there is no general analytical method for determining the optimal value for γ, some numerical experimentation (*trial-and-error*) is required. Sena & Toksöz (1990) suggest the use of the total data error in each iteration as the regularization parameter. As the iteration proceeds toward convergence, γ decreases. Another approach (Gull & Daniel, 1978) is to select the regularization parameter that approximates the statistics $\Sigma_{j,m} (\Phi^E_{j,m} - \Phi^C_{j,m})^2/\sigma^2_{j,m}$ to its expected value, the total number of observations ($N_y M$), assuming that the data have gaussian errors with standard deviation $\sigma_{j,m}$. Other methods for choosing the regularization parameter, in the context of image restoration, are reviewed by Galatsanos & Katsaggelos (1992).

Optimization Algorithm

The minimization of the objective function $J(\mathbf{p})$ given by equation (21), subjected to simple bounds on **p**, is solved using a first-order optimization algorithm – E04UCF routine – from the NAG Fortran Library (1993). This routine is designed to minimize an arbitrary smooth function subject to constraints (simple bounds, linear nonlinear constraints), using a sequential programming method. For the n-th iteration, the calculation proceeds as follows:

1. Solve the forward problem for $\mathbf{p}^n$ and compute the objective function $J(\mathbf{p}^n)$.
2. Compute by finite differences the gradient $\nabla J(\mathbf{p}^n)$.
3. Compute a positive-definite quasi-Newton approximation to the Hessian $\mathbf{H}^n$:

$$\mathbf{H}^n = \mathbf{H}^{n-1} + \frac{\mathbf{b}^n(\mathbf{b}^n)^T}{(\mathbf{b}^n)^T\mathbf{u}^n} - \frac{\mathbf{H}^{n-1}\mathbf{u}^n(\mathbf{u}^n)^T\mathbf{H}^{n-1}}{(\mathbf{u}^n)^T\mathbf{H}^{n-1}\mathbf{u}^n},$$

   where $\mathbf{b}^n = \mathbf{p}^n - \mathbf{p}^{n-1}$,
   $\mathbf{u}^n = \nabla J(\mathbf{p}^n) - \nabla J(\mathbf{p}^{n-1})$.
4. Compute the search direction $\mathbf{d}^n$ as a solution of the following quadratic programming subproblem:
   Minimize $(\mathbf{g}^n)^T\,\mathbf{d}^n + \frac{1}{2}(\mathbf{d}^n)^T(\mathbf{H}^n)\,\mathbf{d}^n$
   subject to $l_q - p_q^n \le d_q \le u_q - p_q^n$,
   where $\mathbf{g}^n = \nabla J(\mathbf{p}^n)$.
5. Set $\mathbf{p}^{n+1} = \mathbf{p}^n + \beta^n\,\mathbf{d}^n$, where the step length β^n minimizes $J(\mathbf{p}^n + \beta\mathbf{d}^n)$.
6. Test the convergence: stop, if **p** satisfies the first-order Kuhn-Tucker conditions (Powell, 1974) and $\beta\,\|\,\mathbf{d}\,\| < \sqrt{\epsilon}\,(1 + \|\,\mathbf{p}\,\|)$, where ε specifies the accuracy to which one wishes to approximate the solution of the problem; otherwise, return to step 1.

NUMERICAL RESULTS

The numerical method presented in the previous sections was tested over different earth models, using synthetic data. In all simulations, the conductive half-space (Ω+, see Fig. 1) was cellularized into 8 x 11 blocks, with $\Delta y = 10\ km$ and Δz varying from 1 to 10 km. MT data (real and imaginary parts of H_x) was generated by the forward model, using the same mesh of the inversion scheme, at 11 stations at $z = 0$, and at 20 logarithmically spaced frequencies ranging from 0.0001 to 0.01 Hz. To simulate experimental errors, a one percent Gaussian noise was added to the exact data. The computations were performed until convergence was attained, by using a uniform conductivity σ+ half-space as the starting model.

Results are presented in the form of two-dimensional conductivity maps in logarithmic scale. The unknown conductivity values were put into **p** by a vertical rasterscan on the two-dimensional maps, starting from the left top corner. The leftmost column (boundary condition) and the topmost row (earth's surface) are assumed to be known and, therefore, were left out of the inversion procedure.

The MINENT-1 inversion method was first applied to a structure consisting of a conductive prism Ω^c and a resistive prism Ω^r, both embedded in the half-space Ω^+, with a conductivity ratio of $\sigma^c/\sigma^+ = 10$ and $\sigma^r/\sigma^+ = 0.1$. Numerical results were computed considering the following test cases: (1) no regularization; (2) MINENT-1 regularization; (3) and (5) MAXENT-0 regularization; and (4) MAXENT-0 and MINENT-1 regularization. The values of the regularization parameters have been set by numerical experimentation.

Conductivity maps, in logarithmic scale, are displayed in Fig. 4a through 4f, showing the true model used to generate the synthetic data and the four cases. For each test case, Tab. 1 also presents the number of iterations until final convergence I_f, the normalized *rms* residue, $\rho = R(\mathbf{p})/R(\mathbf{p}^0)$, the normalized entropies $\bar{S}_0$ and $\bar{S}_1$, as well as the normalized *rms* error defined by

$$\epsilon = \left[\sum_{q=1}^{Q} (p_q - p_q^{exact})^2 / (p_q^0 - p_q^{exact})^2 \right]^{1/2} \qquad (26)$$

Figure 4c shows that the MINENT-1 inversion algorithm properly recovered the conducdtive distribution. The combination of both regularization techniques into an hybrid approach, displayed in Fig 4e, entailed a slight degradation of the solution when compared to the results in Fig. 4c. On the other hand, the reconstructions 4b and 4d were contaminated by artifacts. Particularly, Fig. 4d seems to indicate that γ_0 should be increased in order to improve the MAXENT-0 regularization. However, a bigger value for the regularization parameter in this case only enhances the filtering of low entroy structures in the inverse solution, removing artifacts but also valuable information, as shown in Fig. 4f. Even increasing considerably the level of noise added to the data (from 1 to 8%), the MINENT-1 method still yields good results, as seen in Fig. 5, illustrating the robustness of the proposed inversion algorithm.

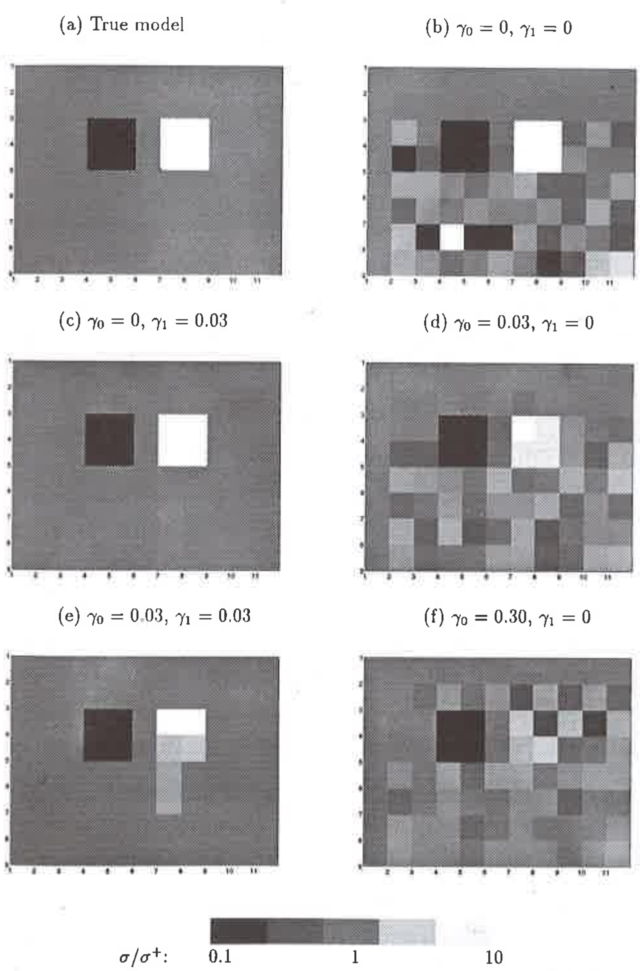

Figure 4 - Conductivity maps in logarithmic scale.

Figura 4 - *Mapas de condutividade em escala logarítmica.*

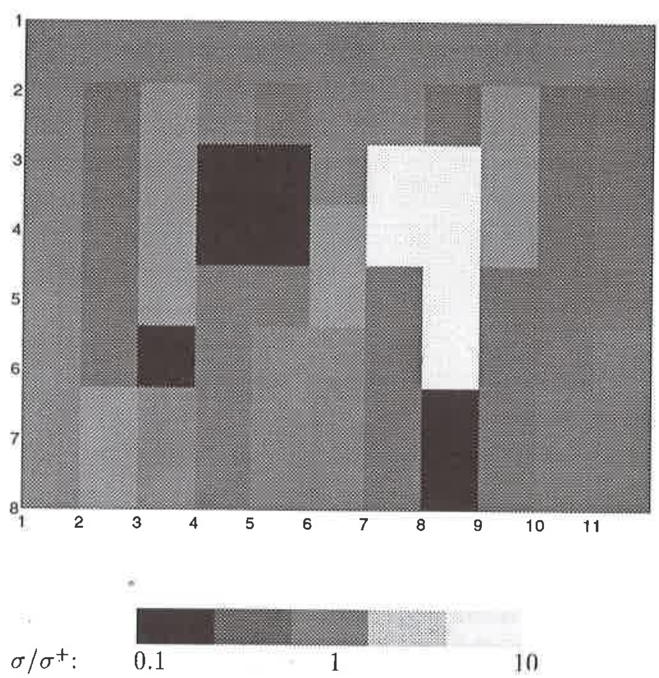

Figure 5 - Conductivity map in logarithmic scale; $\gamma_0 = 0$ e $\gamma_1 = 0.50$, data with 8% gaussian noise (true model shown in Fig. 4a).

Figura 5 - *Mapa de condutividade em escala logarítmica;* $\gamma_0 = 0$ e $\gamma_1 = 0{,}50$, *dados com 8% de ruído gaussiano (modelo exato apresentado na Fig. 4a).*

Test case	Figure	γ_0	γ_1	I_f	ϵ	ρ	$\bar{S}_0$	$\bar{S}_1$
1	4b	0.00	0.00	88	0.6355	0.0210	0.8536	0.7953
2	4c	0.00	0.03	210	0.0078	0.0233	0.8791	0.4054
3	4d	0.03	0.00	70	0.3134	0.0222	0.9003	0.8123
4	4e	0.03	0.03	176	0.5095	0.0272	0.9160	0.4726
5	4f	0.30	0.00	138	0.8000	0.0280	0.9575	0.8266

Table 1 - Numerical results for test cases of Fig. 4.

Tabela 1 *- Resultados numéricos para os casos teste da Fig. 4.*

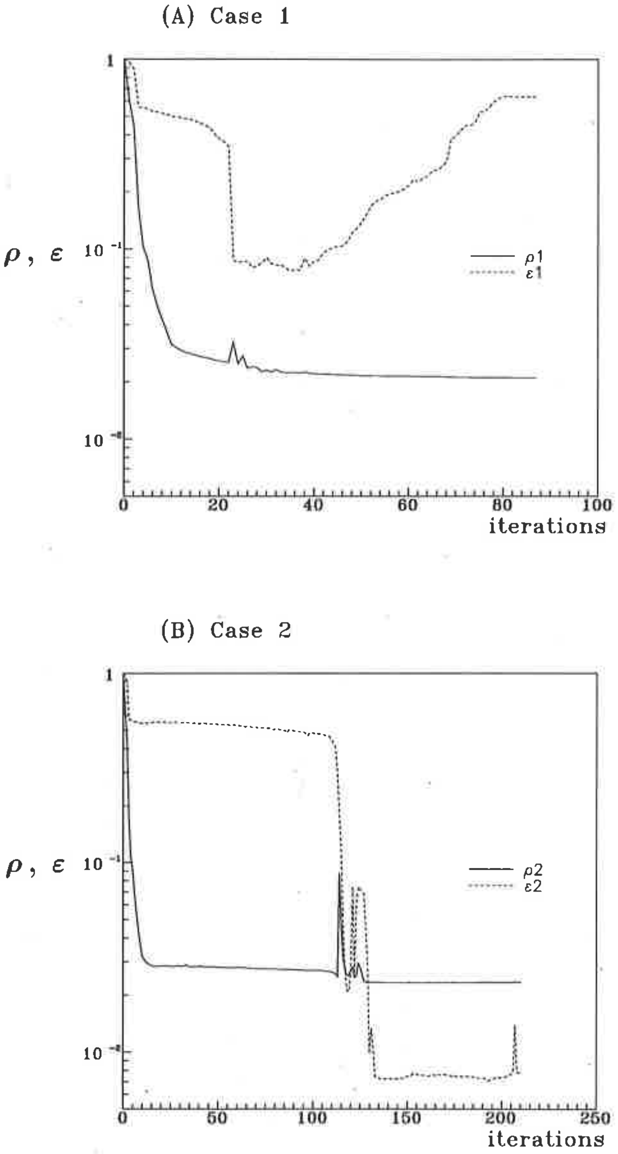

Figure 6 - Error ϵ and residue ρ versus the iteration number for test cases 1 and 2.

Figura 6 *- Erro ϵ e resíduo ρ em função do número de iterações para os casos teste 1 e 2.*

A comparison of entropy results in Tab. 1 indicates that, while the zeroth-order entropy values span over a relatively narrow range ($0.85 < \bar{S}_0 < 0.96$), the first-order entropy figures have a much higher variability ($0.41 < \bar{S}_1 < 0.83$), the lowest levels being associated to the best reconstructions. This result suggests that the MINENT-1 regularization technique constrains the class of possible solutions into a restricted set of low entropy models, constituted by locally smooth regions separated by sharp discontinuities.

Figures 6a and 6b display ϵ and ρ as a function of iteration, for test cases 1 (no regularization) and 2 (MINENT-1 regularization). In the absence of any regularization, as iteration proceeds, the inversion procedure overfits the data, degrading the inverted model and, thus, increasing the value of ϵ. In contrast, the regularization scheme in case 2 assures a monotonic reduction of the error. However, the converged value of ρ is smaller in case 1 than in case 2 (see Tab. 1), which perfectly illustrates the trade-off between entropy and residue performed by the MINENT-1 method.

To further compare the MAXENT-0 and MINENT-1 methods, two different configurations (models *a* and *b*) were considered, respectively depicted in Figs. 7a and 7b. Configuration *a* has relatively low zeroth-order entropy content ($\bar{S}_0^a = 0.8558$), and consists of a conductive prism Ω^1 embedded in a half-space Ω^+, with $\sigma^1/\sigma^+ = 10$. The second model depicts a half-space Ω^+ with a resistive inclusion Ω^2 ($\sigma^2/\sigma^+ = 0.1$). and, as opposed to the first test case, has a zeroth-order entropy value close to its maximum ($\bar{S}_0^b = 0.9977$). Both examples have low first-order entropy levels ($\bar{S}_1^a = 0.5420$ and $\bar{S}_1^b = 0.1632$).

As expected, the MAXENT-0 method gave an excellent result (Fig. 7f) when applied to model *b*, the only one with a high $\bar{S}_0$ level. Although the true model is still evident in Fig. 7e, the reconstruction was heavily degraded by spurious structures. As already seen in the previous example (Fig. 4f), a further increase in the value of γ_0 will only lead to an unnecessary loss of resolution, without enhancing the overall quality of the reconstructed model. These results clearly indicate that maximizing $\bar{S}_0$ may not be the best approach when looking for low entropy models.

In comparison, the MINENT-1 method properly recovered models *a* and *b*, as presented in Figs 7c and 7d. These results show that, when there is prior evidence about the low entropy content of the true models, the MINENT-1 regularization scheme allows to introduce a certain degree of roughness into the inverse solutions, while preventing them to be contaminated by artifacts. This feature is not shared by the classical regularization schemes, which maximize smoothness for some tolerable level of misfit to the data (Smith & Brooker, 1988; Gull & Daniel, 1978). For instance, results similar to those displayed in Fig. 4c may only be obtained by Occam's inversion if the *exact* placement of the sharp discontinuities in conductivity is known *a priori* (deGroot-Hedlin & Constable, 1990).

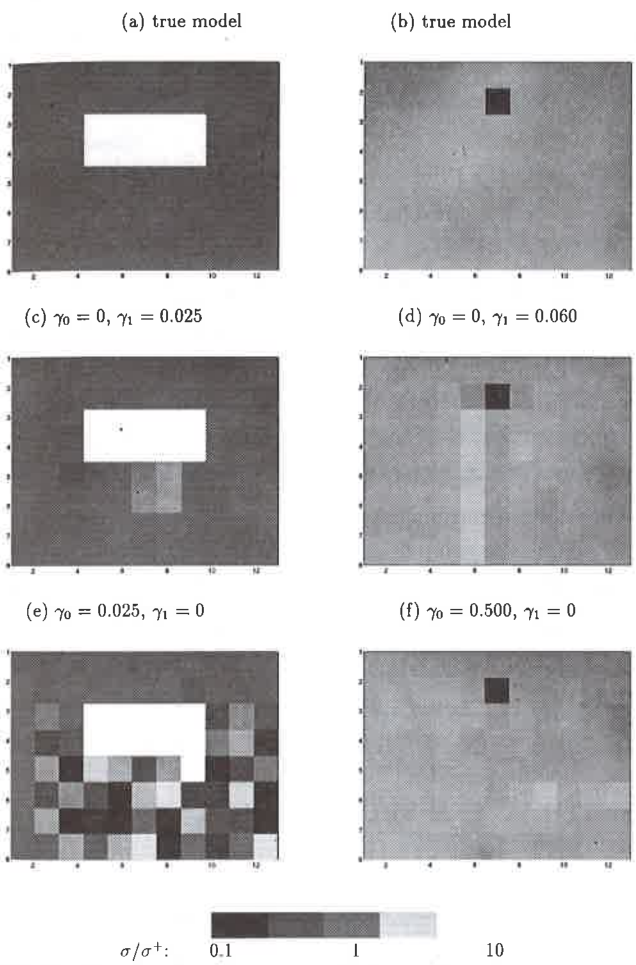

Figure 7 - Conductivity maps in logarithmic scale.

***Figura 7** - Mapas de condutividade em escala logarítmica.*

Model	Figure	γ_0	γ_1	If	$\in$	ρ	$\bar{S}_0$	$\bar{S}_1$
a	7c	0.000	0.025	43	0.0667	0.0157	0.8630	0.5925
	7c	0.025	0.000	126	0.6533	0.0146	0.9026	0.9039
b	7d	0.000	0.060	100	0.9829	0.1190	0.9969	0.5190
	7f	0.500	0.000	20	0.5547	0.1019	0.9974	0.8465

Table 2 - Numerical results for test cases of Fig. 7.

***Tabela 2** - Resultados numéricos para os casos teste da Fig. 7.*

CONCLUSIONS

The data from an electromagnetic experiment constitute a blurred image of the earth structure (Oldenburg, 1990). In this paper, a new inversion technique, called the minimum first-order entropy (MINENT-1) method, was proposed for the reconstruction of two dimensional geoelectric conductivity distributions from MT data. The method combines an iterative search with a regularization technique based on the assignment of an entropy measure to the vector of first-differences of the unknown conductivities.

Numerical simulations, using synthetic data corrupted with gaussian noise, have shown that the MINENT-1 algorithm converged to excellent 2D earth models, yielding in many cases results that are superior to those obtained by the maximum entropy formalism. These results suggest that, unlike other classical regularization schemes, which maximize smoothness for a given data, the proposed method constrains the class of possible solutions into a restricted set of low entropy models, constituted by locally smooth regions separated by sharp discontinuities. Many geophysically interesting properties and structures may behave in a similar fashion.

In summary, the MINENT-1 method is an effective approach for the incorporation of prior information about the local smoothness of the true physical model. Natural extensions of the present work include the development of an accurate three-dimensional forward model for dealing with field data, and the improvement of the computational efficiency of the algorithm.

ACKNOWLEDGEMENTS

The authors express their gratitude to Drs. A. L. Padilha and N. B. Trivedi, from CEA/INPE, whose support greatly contributed to this paper. The authors recognise the role played by FAPESP, São Paulo State Foundation for Research Support, in supporting this piece of work through a Thematic Project grant (Process 96/07200-8).

REFERENCES

DE BOISSIEU, PAPOULAR, R. J. & JANOT, C. - 1991 - Maximum entropy method as applied in quasi-crystallography. Europhysics Letters, **16**: 343-347.

CAGNIARD, L. - 1953 - Basic theory of the magnetotelluric method of geophysical prospecting. Geophysics, **18**: 605-635.

CONSTABLE, S. C., PARKER, R. L. & CONSTABLE, G. C. - 1987 - Occam's inversion: A practical algorithm for generating smooth models from electromagnetic sounding data. Geophysics, **52**(3): 289-300.

DEGROOT-HEDLIN, C. & CONSTABLE, S. - 1990 - Occam's inversion to generate smooth, two-dimensional models from magnetotelluric data. Geophysics, **55**(12): 1613-1624.

NAG FORTRAN LIBRARY - 1993 - Mark 16, Oxford, UK.

FLEISHER, M., MAHLAB, U. & SHAMIR, J. - 1990 - Entropy optimized filter for pattern recognition. Applied Optics, **29**: 2091-2098.

GALATSANOS, N. P. & KATSAGGELOS, A. K. - 1992 - Methods for choosing the regularization parameter and estimating the noise variance in image restoration and their relation. IEEE Transactions on Image Processing, **1**(3): 322-336.

GULL, S. F. & DANIELL, G. J. - 1978 - Image reconstruction from incomplete and noisy data. Nature, **272**: 686-690.

HOFFMAN, J. D. - 1993 - Numerical methods for engineers and scientists, McGraw-Hill Book Co., Singapore.

JAYNES, E. T. - 1957 - Information theory and statistical mechanics. Physical Review, **106**: 620-630.

JAYNES, E. T. - 1982 - On the rationale of the maximum entropy methods. Proceedings of the IEEE, **70(9)**: 939-952.

JONES, F. W. & PRICE, A. T. - 1970 - The perturbatioins of alternating geomagnetic fields by conductivity anomalies. Geophys. J. R. Astr. Soc., **20**: 317-334.

JUPP, D. L. B. & VOZOFF, K. - 1977 - Two-dimensional magnetotelluric inversion. Geophys. J. R. Astr. Soc., **50**: 333-352.

MADDEN, T. R. & MACKIE, R. L. - 1989 - Three-dimensional magnetotelluric modeling and inversion. Proceedings of the IEEE, **77**(2): 318-333.

OLDENBURG, D. - 1990 - Inversion of electromagnetic data: An overview of new techniques. Surv. Geophys, **11**: 231-270.

OLDENBURG, D. & ELLIS, R. G. - 1991 - Inversion of geophysical data using an approximate inverse mapping. Geophys. J. Int., **105**: 325-353.

PILKINTON, M. & TODOESCHUCK, J. P. - 1991 - Naturally smooth inversions with a priori information from well logs. Geophysics, **56**(11): 1811-1818.

PHILLIPS, D. L. - 1962 - A technique for the numerical solution of certain integral equations of the first kind. Journal of ACM, **9**: 85-97.

POWELL, M. J. D. - 1974 - Introduction to Constrained Optimization. In: Numerical Methods for Constrained Optimization, Gill P. E. and Murray W. (Eds.), Academic Press, London and New York, pp. 1-28.

RAICHE, A. - 1994 - Modeling and inversion – Progress, problems and challenges. Surv. Geophys., **15**: 159-207.

RAMOS, F. M. & GIOVANNINI, A. - 1995 - Résolution d'un problème inverse multidimensionnel de diffusion de la chaleur par la méthode des eléments analytiques et par le principe de l'entropie maximale. International Journal of Heat and Mass Transfer, **38**: 101-111.

SENA, A. G. & TOKSÖZ, M. N. - 1990 - Simultaneous reconstruction of permittivity and conductivity for crosshole geometries, Geophysics, **55**(10): 1302-1311.

SHANNON, C. E. & WEAVER, W. - 1949 - The Matemathical Theory of Communicatioin, Univ. of Illinois Press, Urbana.

SMITH, J. T., & BROOKER, J. R. - 1988 - Magnetotelluric inversion for minimum structure. Geophysics, **53**(12): 1565-1576.

SMITH, J. T. & BROOKER, J. R. - 1991 - Rapid inversion of two- and three-dimensional magnetotelluric data. Journal of Geophysical Research, **96**(B3): 3905-3922.

SMITH, R. T., ZOLTANI, C. K., KLEM, G. J. & COLEMAN, M. W. - 1991 - Reconstruction of tomographic images from sparse data sets by a new finite element maximum entropy approach. Applied Optics, **30**: 573-582.

TIKHONOV, A. N. - 1950 - On determining electrical characteristics of the deep layers of the earth's crust. Dokl. Akad. Nauk. USSR, **73**: 295-297.

TIKHONOV, A. N. - 1963 - Solution of incorrectly posed problems. Soviet Math. Dokl, **4**: 1624-1627.

TIKHONOV, A. N. & ARSENIN, V. Y. - 1977 - Solutions of ill-posed problems, John Wiley & Sons, New York.

TWOMEY, S. - 1963 - On the numerical solution of Fredholm integral equations of the first kind by inversion of the linear system produced by quadrature. Journal of ACM, **10**: 97-101.

Submetido em: 01/10/96.
Revisado pelo(s) autor(es) em: 04/07/97.
Aceito em: 10/07/97

INVERSÃO NUMÉRICA DE DISTRIBUIÇÕES BIDIMENSIONAIS DE CONDUTIVIDADE GEOELÉTRICA A PARTIR DE DADOS MAGNETOTELÚRICOS

Campos eletromagnéticos induzidos por fontes naturais da ionosfera e da magnetosfera para determinar a condutividade elétrica da Terra têm uma ampla aplicação em geofísica, tais como prospecção de petróleo e de água no subsolo, e mineração. Este problema inverso, também conhecido como inversão magnetotelúrica (MT), é particularmente importante em regiões em que a análise com os métodos sísmicos convencionais é difícil.

Algoritmos de inversão de dados MT comumente envolvem uma busca sistemática de um *modelo de solo* que melhor ajuste os dados observados. O processo de inversão consiste na minimização de uma função objetivo, que inclui a diferença quadrática entre os dados calculados pelo modelo numérico (matemático) e os dados observados, e uma função de regularização. O termo de regularização expressa uma informação adicional sobre a geologia do sistema, o que permite estabilizar a resposta do modelo inverso, pois problemas inversos são tipicamente instáveis, o que pode ocasionar soluções espúrias sob a presença de ruídos. Nos métodos clássicos de regularização, desenvolvidos por Phillips (1962), Tikhonov (1963) and Twomey (1963), soluções ótimas são obtidas com a ajuda de um operador de *suavização*, que essencialmente calcula a primeira e a segunda derivadas numéricas das condutividades.

Neste trabalho propõe-se uma nova técnica de inversão, chamada de método da mínima entropia de primeira ordem (MINENT-1), para reconstrução de distribuições bidimensionais de condutividade geoelétrica, a partir de dados magnetotelúricos (MT). O método combina uma busca iterativa com uma técnica de regularização baseada na minimização da medida de entropia do vetor de diferenças primeiras das condutividades a serem estimadas. Simulações numéricas, com a utilização de dados sintéticos contaminados com ruído gaussiano, mostram que o algoritmo MINENT-1 produz excelentes reconstruções de condutividade, com resultados melhores que os obtidos pelo método da máxima entropia. Diferentemente dos outros esquemas clássicos de regularização, que maximizam suavidade para um determinado conjunto de dados, o método proposto limita a classe de possíveis soluções a um cojunto restrito de modelos de baixa entropia, constituído por regiões localmente lisas separadas por discontinuidades abruptas. Esta abordagem pode ser bastante eficaz para incorporação de informação *a priori* sobre a natureza da suavidade local do modelo físico real.

NOTES ABOUT THE AUTHORS
NOTAS SOBRE OS AUTORES

Haroldo Fraga de Campos Velho

Received a B. S. in Chemical Enginneering from the Pontifícia Universidade Católica do Rio Grande do Sul (PUCRS), Brazil, in 1982, a D.Sc. and M.Sc. degree in Mechanical Engineering from the Universidade Federal do Rio Grande do Sul (UFRGS), Brazil, in 1992 and 1988, respectively. He is currently a researcher of the Computing and Applied Mathematics Laboratory (LAC) at National Institute for Space Research (INPE). His research interests include turbulence and data initialization/assimilation in atmospheric models, inverse problems, and scientific computing.

Fernando Manuel Ramos

Received a B. S. in Mechanical-Aeronautical Engineering from the Instituto Tecnológico de Aeronáutica (ITA), Brazil, in 1981, a M. Sc. degree in Space Sciences from the Instituto Nacional de Pesquisas Espaciais (INPE), Brazil, in 1986, and a Diploma of Advances Studies and a Doctorate degree in Mechanical Fluids from the Ecole Nationale de l'Aéronautique et de l'Espace (ENSAE), France, in 1988 and 1992, respectively. He is currently a senior researcher of the Computing and Applied Mathematics Laboratory (LAC) at INPE. His research interests include inverse problems, heat transfer and scientific computing.